Optimal location and minimum number of superconducting fault current limiters for the protection of power grids

Xiuchang Zhang, H. S. Ruiz, Jianzhao Geng, and T. A. Coombs

***Abstract*—This paper presents a novel method to determine the optimal strategy for the allocation of multiple resistive superconducting fault current limiters (SFCLs) aiming to improve the overall protection of standard power grids. The presented approach allows for the straightforward determination of the optimal resistance of the SFCL, accounting for short circuit events occurring at different locations, by modelling the electro-thermal properties of the SFCL via a temperature dependent $E-J$ power law. This material law, based on previous experimental evidence, allows for the introduction of flux pinning, flux creep, and flux flow properties of the superconducting material within a minimum level of complexity. Thereby, we have observed a distinctive kink pattern in the current limiting profiles of the SFCLs, from which no further reduction of the first peak of the fault current is achieved when a greater resistance is considered, allowing a univocal determination of the optimum SFCL resistance. This peculiarity is not observed when the model for the quench properties of the SFCL is simplified towards an exponential resistance, although the last can be used as an auxiliary process for addressing the first guess on the resistance value required for a specific strategy, as it demands less computing time. We have also determined that for many of the cases studied, i.e., for the combinations between one or more SFCLs installed at different locations, and those subjected to fault events located at different points in the network, the recovery time of the superconducting properties of at least one of the SFCLs can last for more than 5 mins, constraining the feasibility of a large-scale deployment of this technology. However, by assuming that the practical operation of the SFCL is assisted by the automatic operation of a bypass switch when the SC material is fully quenched, we have determined that the optimal strategy for the overall protection of power grids of standard topology requires a maximum of three SFCLs, with recovery times of less than a few seconds. This information is of remarkable value for power system operators, as it can establish a maximum investment threshold which ultimately can facilitate making decisions regarding the deployment of SFCL technologies.**

***Index Terms*—Superconducting fault current limiter, Fault protection, Optimal location, Electrical power grid, Optimal resistance**

I. Introduction

EXPANSION of distributed generation, grid interconnection, and the always growing demand of electric power are leading to the power network operators to consider upgrading the fault protection systems [1]. We know that under certain circumstances, the extremely high fault current levels could lead to failure of the traditional protection devices (e.g. circuit breakers), which may then result in severe damage to costly on-grid equipments [2], [3], [4]. During the normal operation of a power system, superconducting fault current limiters (SFCLs) have the advantage of being almost invisible. However, in cases of short circuit events, the fast transition from the superconducting state towards a highly resistive state, known as *quench*, allows the SFCL to reduce the first peak of the fault current to an acceptable level [5]. Moreover, the SFCL can automatically recover its superconducting state after the clearance of the fault [6].

SFCLs can be categorized into three types, namely resistive, inductive and hybrid [7]. In this paper, we focus on the resistive type SFCL. Power system studies have hitherto discussed the performance and optimal location of a single SFCL [8], however, comprehensive research activities about cooperation of multiple SFCLs have yet to be analysed in detail. Hence, studying the optimal number and installing strategies of SFCLs in a complex grid model is the main concern of this work. To achieve this goal, we built a power system model according to the UK network standards [9], in which different types of power generations and loads were included. We consider this model representative and could be expanded into even larger scale networks. For the simulation of resistive SFCLs, two SFCL models were developed based on commonly used methods: the first approach was to utilise an exponential equation to describe the generated impedance during faults [10], while the other implemented a more realistic temperature-dependant $E-J$ power-law [11]. Simulation results showed three SFCLs needed to be installed to achieve desired protection for the entire system. In addition, it was illustrated that, compared with the $E-J$ power-law SFCL model, the $e-$model had certain limitations due to lack of consideration about material physical properties, and therefore was not accurate enough for SFCL performance simulations.

II. Power grid configuration and SFCL models

A. System configuration

The designed power system model shown in Fig. 1 contains a wind power plant the specifications of which were chosen according to the Scottish onshore wind farm Crystal Rig 2&2a [12]. After supplying power to industrial load 1

This work was supported by the Engineering and Physical Sciences Research Council (EPSRC) under grant NMZF/064. Xiuchang Zhang acknowledges a grant from the China Scholarship Council (No. 201408060080).

The authors are with Department of Engineering, University of Cambridge, 9 JJ Thomson Avenue, Cambridge CB3 0FA, United Kingdom (e-mail: xz326@cam.ac.uk).

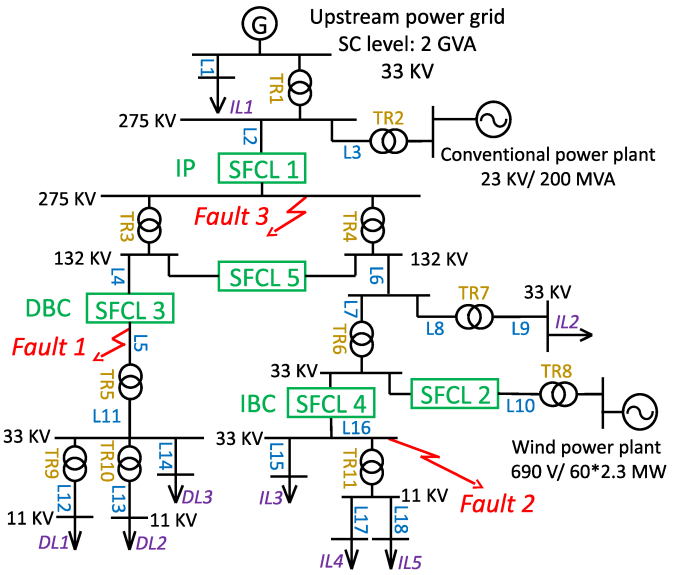

Fig. 1. Power grid model considered into this study. The power system's structure is thoroughly discussed in Sec. II-A.

TABLE I
PARAMETERS OF LOADS, TRANSFORMERS AND TRANSMISSION LINES

Loads (MW)		Transformers (MVA)		Transmission Lines (km)			
DL1	20	**TR1&2**	250	**L1&8**	4	**L11**	12
DL2	30	**TR3&5**	220	**L2**	70	**L12**	2
DL3	50	**TR4&6**	200	**L3&4**	20	**L13**	1
IL1	80	**TR7**	120	**L5**	30	**L14**	6
IL2	70	**TR8**	180	**L6**	80	**L15**	5
IL3	55	**TR9**	40	**L7**	10	**L16**	15
IL4	30	**TR10**	60	**L9**	1	**L17**	4
IL5	30	**TR11**	90	**L10**	10	**L18**	2

(IL1), the upstream power grid with 2 GVA short-circuit level is connected with a 200 MVA conventional power plant. Then, the power flows downwards to domestic (at left) and industrial (at right) branches, simultaneously. The domestic branch contains three domestic loads (DL1, DL2, and DL3), while the industrial branch has four industrial loads (IL2 to IL5) connected. In addition, a wind farm which consisting of 60 induction type wind turbines each rating at 2.3 MVA is integrated on the right side of the power grid (between IL2 and IL3-5).

Three prospective locations of three-phase to ground short circuit events, which represent contingencies at the domestic branch (Fault 1), industrial branch (Fault 2), and high voltage transmission line (Fault 3), have been simulated. The performance study is pursued taking into consideration both sole SFCL strategies and multiple installation schemes of up to five SFCLs, located at the outgoing feeder of the conventional (SFCL 1) and wind (SFCL 2) power plants, the ports of the domestic (SFCL 3) and industrial (SFCL 4) branches, and the bus-tie coupling the domestic and industrial branches (SFCL 5). Detailed information about the parameters of the system is listed in Table I.

B. Exponential-resistance SFCL model

The quench transition of the SFCL is equivalent to the insertion of a high impedance into the power system. During normal operation, the impedance of the SFCL of the system is negligible, i.e., before the occurrence of a fault event at $t = t_f$ and, also after its full clearance plus the time elapsed for recovering the superconductor properties, $t > (t_{cf} + t_r)$. A reasonable assumption is to consider that under these regimes the SFCL acts as a single resistance defined by $R_n = 10^{-6}\ \Omega$ [10], [13]. Once a fault occurs and is detected by the SFCL, the SFCL swiftly develops an increasing resistance until the fault is cleared at the time $t^* = t_{cf}$. This behaviour can be modelled by an exponential law ($e-$law) as follows [14], [15].

$$R(t) = \begin{cases} R_n \quad , \quad \in Normal\ Con., \\ R_m \left[1 - exp\left(-\dfrac{t^* - t_f}{t_{sc}}\right)\right], \in Fault\ Con., \end{cases} \tag{1}$$

where R_m represents the maximum resistance of the quenched superconducting (SC) material. A quenching constant time, $t_{sc} = 1$ ms, is introduced according to [16] & [17]. Before the fault is cleared ($t_f \leq t \leq t_{cf}$), the SFCL resistance R_m can be calculated by setting $t^* = t$ in Eq. 1. Then, during the recovering period ($t_{cf} \leq t < t_{cf} + t_r$) of the superconducting properties, $t^* \equiv t_{cf}$. Finally, after recovery of the SFCL, the normal condition of the power grid is then restored.

C. E-J power law based SFCL model

Rather than using predefined parameters as in the exponential-resistance SFCL model ($e-$law model), under the framework of the $E - J$ power law, the quench and recovery properties of the SFCL are determined by the thermal and electrical properties of the SC material within the real time conditions of the power grid. Recently, we have introduced [18] a temperature dependent three-stage SFCL model based upon the well known $E - J$ power law for the flux pinning and flux flow stages of the SFCL, and Ohm's law for describing its normal (no-superconducting) stage [11]. In order to obtain the instantaneous temperature values of the SC material and then get the response of the overall system, a first order approximation of the heat transfer between the superconductor and liquid nitrogen has been implemented. Earlier experimental evidence has shown that the power factor in the $E-J$ power law that describes the flux pinning and flux flow regimes may also obey a temperature dependent function [19], [20], [21]. This fact helps to unify the flux pinning and flux flow regimes into a single superconducting stage as recently proposed in [22]. Thus, by taken into consideration the previous statements for the SFCL, in this paper the core of the $E-J$ power law based model for temperatures lower than the critical temperature of the SC ($T_c(Bi2212) = 85$ K) [23], and greater than the liquid Nitrogen temperature at 1 atm ($T_0 = 77$ K) refers to:

$$E\left(T(t)\right) = E_0 \left(\frac{J_c(T_0)}{J_c(T(t))} \frac{(T_c - T_0)}{(T_c - T(t))}\right)^{n(T(t))}, \tag{2}$$

with

$$n\left(T(t)\right) = (n_0 - 1)\left(\frac{T_c - T(t)}{T_c - T_0}\right)^{1/4} + 1, \tag{3}$$

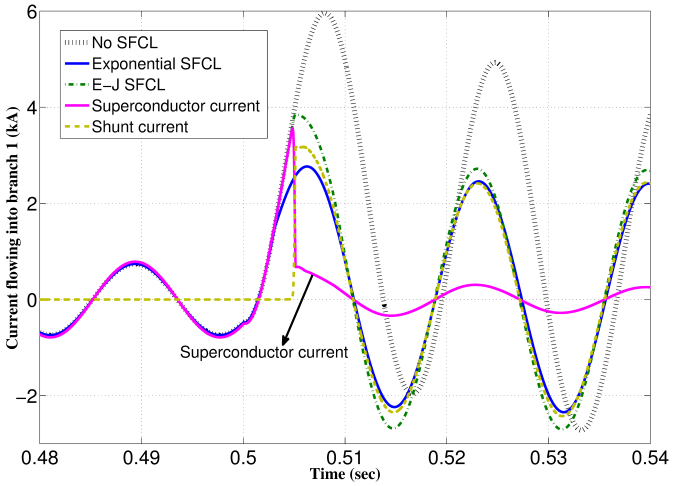

Fig. 2. (Color Online) Fault-current limiting dynamics of SFCL-3 responding to Fault-1 (see Fig. 1) under e law and $E-J$ power law models. The current sharing profile between the SC and the shunt resistance of the $E-J$ power law SFCL model is also displayed.

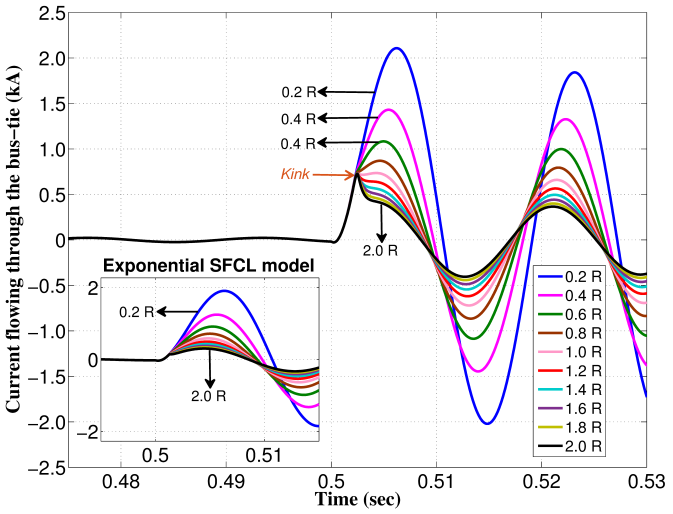

Fig. 3. (Color Online) Limited current of SFCL-5 responding to Fault-2 (see Fig. 1) as a function of its maximum rated resistance $R_m = 0.2R_m^\dagger, 0.4R_m^\dagger, ..., 2R_m^\dagger$, with $R_m^\dagger = 25\Omega$, under the $e-$law (inset) and the $E-J$ power law models.

where the standard parameters $E_0 = 1\ \mu V/cm$, $J_c(T_0) = 12\ MA/m^2$, $n_0 = 9$, chosen in good agreement with the experimental data reported in [19] and [24].

Finally, in order to improve the recovery characteristics of the SFCL, a shunt resistance (R_s) is connected in parallel with the superconductor [24] for both SFCL models. The function of the shunt resistance is to ease the thermal and electrical stresses of the SC material after quenching.

III. Performance Comparison between the Implemented SFCL Models

In order to compare the current limiting performance of the above described SFCL models, below we show the results obtained when a 200 ms three-phase to ground fault is initialized at the domestic branch (Fault 1), at $t_f = 0.5$ s, with SFCL installed at location 3 (Fig. 1). As illustrated in Fig. 2, the first peak of the prospective fault current (6 KA) is effectively limited by 55% to 2.7 KA, when the $e-$law model is considered. However, only a $\sim 35\%$ current reduction is seen by the $E-J$ power law model. The 20% difference between the two results shows that the performance of the $e-$law SFCL model significantly overestimates the behavior of the SFCL. This inaccuracy of the $e-$law is due to the excessive growth speed of SFCL resistance, which is caused by ignorance of the temperature dependence.

To illustrate the relationship between the maximum SFCL resistance and the reduction in the first peak of the fault current, Fig. 3 displays the profiles of current flowing through a SFCL that installed at the bus-tie (SFCL 5, $R_m^\dagger = 25\Omega$), when a 200 ms three-phase to ground fault in the domestic branch (Fault 2) is initialized from $t_f = 0.5$ s. Under normal operation of the power grid, the overall system has been regulated such that only a current of 20 A is observed at the bus-tie. However, when a fault event occurs at location Fault 2, the first peak of the short-circuit current can reach up to 4.1 kA. With the installation of a SFCL, when the $e-$law model is considered, and R_m increases from $0.2R_m^\dagger$ to $2R_m^\dagger$, we have obtained that the first peak of the fault current gradually drops from 1.9 kA to 0.3 kA with a backwards displacement of the peak values. However, when the $E-J$ power law model is implemented, a quite distinctive feature at 0.7 kA, which we have called "*kink*", has been obtained for the SFCLs with $R_m > R_m^\dagger$. The appearance of this *kink* implies the existence of an optimal R_m value $(R_m^\dagger)$, which may allow SFCLs' manufacturers assessing the optimal length of required SC material regarding specific needs of a power network.

After identifying the optimal operating conditions of SFCLs through studying the impact of the $E-J$ power law model on the power grid, the recovery time, which refers to the time length that the SFCLs need for restoring the SC capabilities after the clearance of the fault, has been calculated. A By-pass Switch (BS) has been incorporated with the SFCL, in order to reduce its recovery time to less than 3 s under all prospective fault conditions (see Table II). The aim of the BS is twofold [25]: First, it allows isolation of the SFCL from the grid after clearing the fault event, thenceforth reducing the Joule heating on the SC material and likewise reduce t_r. Secondly, once the SC state is recovered, the BS automatically reconnects the SFCL to the live power grid. It is to be noticed that without the external assistance of the BS, the operability of the SFCL cannot be recovered within five or more minutes, implying significant cooling costs and negative influence on the power grid that may jeopardize the actual deployment of this technology.

In addition, since faults can occur anywhere in the grid, assessing the optimal installation strategy of a single or even multiple SFCLs needs to be pursued for achieving a desirable protection of the overall power grid. The results of this study are thoroughly described in the following section.

TABLE II
RECOVERY TIME OF SFCLS WITH*/WITHOUT‡ THE BS STRATEGY

Location, Fault:	1*	1‡	2*	2‡	3*	3‡
SFCL 1	0.71 s	329 s	N/A§	N/A§	0.73 s	370 s
SFCL 2	1.34 s	482 s	1.55 s	529 s	1.63 s	559 s
SFCL 3	0.87 s	320 s	N/A§	N/A§	N/A§	N/A§
SFCL 4	N/A§	N/A§	2.11 s	729 s	N/A§	N/A§
SFCL 5	0.87 s	1.01 s	0.80 s	0.82 s	0.77 s	0.79 s

§ N/A stands for those occasions where faults do not represent hazards at the branches where the SFCLs are installed. Therefore, the SFCLs are not triggered under these conditions.

TABLE III
STRATEGY NUMBER (SNO.) VS SFCLS DEPLOYED (SD)

SNo.	SD	SNo.	SD	SNo.	SD
1	1	**11**	2,4	**21**	1,4,5
2	2	**12**	2,5	**22**	2,3,4
3	3	**13**	3,4	**23**	2,3,5
4	4	**14**	3,5	**24**	2,4,5
5	5	**15**	4,5	**25**	3,4,5
6	1,2	**16**	1,2,3	**26**	1,2,3,4
7	1,3	**17**	1,2,4	**27**	1,2,3,5
8	1,4	**18**	1,2,5	**28**	1,2,4,5
9	1,5	**19**	1,3,4	**29**	1,3,4,5
10	2,3	**20**	1,3,5	**30**	2,3,4,5
				31	ALL

* The table shows the 31 strategies which have been examined under all fault conditions.

IV. OPTIMAL INSTALLATION STRATEGY OF SFCLS

In order to achieve an accurate estimation of optimal strategy for installing the SFCLs, and ensure the overall protection of the power grid under diverse fault conditions, a complete study of combinations between the five most likely SFCL locations has been performed. Specifically, by taking into consideration each SFCL scenario and simultaneous integration of up to five SFCLs (the number of SFCLs used in the model is defined by k), we can select the optimal scheme out of the 31 possible strategies (see Table III). Each one of these strategies is assessed under all three fault conditions illustrated in Fig. 1. Hence a total of 93 different cases have been studied.

Fig. 4 shows the obtained results for the most severe cases among the aforementioned 93 ones, in which performance of both $e-$law and $E-J$ power law SFCL models is plotted. These cases refer to measuring points located at: (a) the integration point (IP) with fault in the domestic branch (Fault 1), (b) IP with fault at the high voltage transmission line (Fault 3), (c) the domestic branch connection (DBC) with fault in the domestic branch (Fault 1), and (d) the industrial branch connection (IBC) with fault in the industrial branch (Fault 2).

The safety requirement is set such that with SFCLs deployed, fault currents under all possible fault conditions should be limited to lower than three times of the corresponding normal current [17] (purple solid line). Fig. 4 illustrates that when the $E-J$ power law model is considered, the optimal number is $k=3$, since with implementation of three SFCLs all requirement can be fulfilled and more SFCLs only bring small improvement in performance. In particular, only two different arrangements, strategies 18 $\{$SFCLs $[1,2,5]\}$ and 19 $\{$SFCLs $[1,3,4]\}$, can provide the desired protection, as can be seen from Table IV.

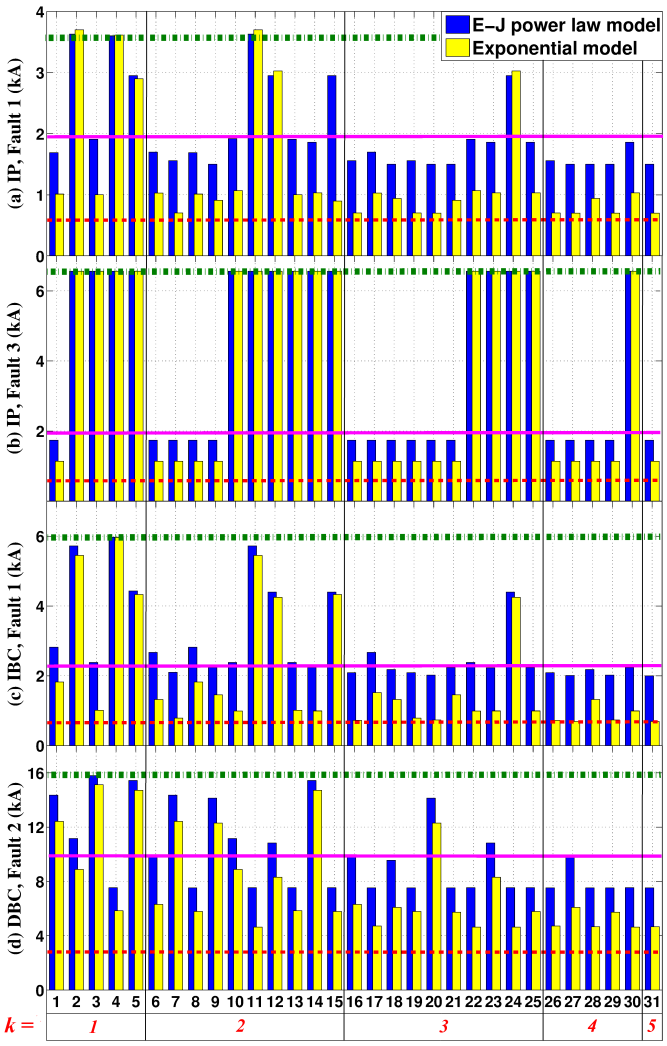

Fig. 4. (Color Online) First peak limiting performance of the 31 installation strategies. Results are shown only for the most hazardous measuring conditions identified in Sec. IV. Red dashed lines represent the normal current levels, and threshold values for safety operation are defined at three times of these values (purple solid lines) [17]. In addition, green dash-dotted lines show the prospective fault current levels without SFCL.

Between the two qualifying options, strategy 18 is more advisable as it includes a direct protection for the wind power plant (SFCL 2) and therefore could prevent potential islanding problems [26]. Moreover, with a SFCL at the bus-tie (SFCL 5), the high loadings and harmonic polluting loads can be directly connected to the MV bus-bars rather than to the HV grid, which means additional savings in transformers needs [27].

In addition, Fig. 4 illustrates that simplified models like the $e-$law can lead to a significant overestimation of the actual SFCLs capabilities. In fact, using the $e-$law SFCL model we have found that seemingly suitable protection conditions can be achieved with the installation of just two SFCLs, as observed for strategies 6 and 8 in Fig. 4. Therefore, despite

the $e-$law model being apparently capable of proving the effectiveness of the SFCLs, this overestimation may cause inaccurate guidance to the system operators. Decision making based on this SFCL model could compromise the stability and reliability of the electrical grid due to the inherent arbitrariness of this material law, where the temperature dynamics is not considered.

V. Conclusion

A comprehensive study about how to determine the number and optimal location strategy for installing single or multiple SFCLs in a UK standard power grid model has been performed. Two different material laws for defining the electrical behaviour of the SC material have been considered. Namely, an exponential resistance model which does not depend on temperature, therefore, relying on the accuracy of preallocated parameters, and secondly, a more sophisticated $E-J$ power law based upon a broad number of experimental observations reported in the literature. We have shown that despite the underlying complexity of the power law, the implementation of simplified models like the $e-$law, inside of a power system simulation environment, is not suitable to be considered as reliable resource for making market decisions. Our conclusion is supported by a thorough analysis of the system performance under three different fault conditions, each considering up to 31 different protection strategies which may include the simultaneous operation of up to five SFCLs. Thus, based on this study we have determined that the minimum number of SFCLs for an effective protection of the entire system is $k = 3$. The most successful strategy is strategy 18, with each SFCL installed at the integrating point (SFCL 1), the wind farm terminal (SFCL 2), and the bus-tie (SFCL 5).

References

[1] M. Fotuhi-Firuzabad, F. Aminifar, and I. Rahmati, " Reliability study of HV substations equipped with the fault current limiter," *IEEE Trans. Power Del.,* vol. 27, pp. 610-617, 2012.

[2] L. Kovalsky, X. Yuan, K. Tekletsadik, A. Keri, J. Bock, and F. Breuer, "Applications of superconducting fault current limiters in electric power transmission systems," *IEEE Trans. Appl. Supercond.,* vol. 15, pp. 2130-2133, 2005.

TABLE IV
Strategy No. (k=3) vs Safety Margin

	IP-Fault 1	IP-Fault 3	IBC-Fault 1	DBC-Fault 2
16	16%	10%	9%	-1%
17	8%	10%	-15%	24%
18	18%	10%	4%	3%
19	16%	10%	9%	24%
20	18%	10%	13%	-41%
21	18%	10%	-2%	24%
22	3%	-233%	-4%	24%
23	5%	-233%	2%	5%
24	-53%	-233%	-48%	24%
25	5%	-233%	-2%	24%

* Safety margin: difference between the threshold value and the limited current, then divided by the safety threshold.

[3] L. Ye, M. Majoros, T. Coombs, and A. Campbell, " System studies of the superconducting fault current limiter in electrical distribution grids," *IEEE Trans. Appl. Supcond.,* vol. 17, pp. 2339-2342, 2007.

[4] H. S. Ruiz, X. Zhang, and T. A. Coombs, "Resistive-Type Superconducting Fault Current Limiters: Concepts, Materials, and Numerical Modeling," *IEEE Trans. Appl. Supercond.,* vol. 25, p. 5601405-5601410, 2015.

[5] J.-C. Llambes, D. W. Hazelton, C. S. Weber, "Recovery under load performance of 2nd generation HTS superconducting fault current limiter for electric power transmission lines," *IEEE Trans. Appl. Supercond.,* vol. 19, pp. 1968-1971, 2009.

[6] S.-W. Yim, H.-R. Kim, O.-B. Hyun, and J. Sim, "Quench and recovery characteristics of Au/YBCO thin film type SFCL," *Physica C,* vol. 463, pp. 1172-1175, 2007.

[7] M. Noe and M. Steurer, "High-temperature superconductor fault current limiters: concepts, applications, and development status," *Supercond. Sci. Technol.,* vol. 20, pp. R15-R29, 2007.

[8] U. A. Khan, J. Seong, S. Lee, S. Lim, and B. Lee, "Feasibility analysis of the positioning of superconducting fault current limiters for the smart grid application using simulink and simpowersystem",*IEEE Trans. Appl. Supercond.,* vol. 21, pp. 2165-2169, 2011.

[9] "UK Electricity Networks," *Parliamentary Office of Science and Technology,*, number 163, October, 2001.

[10] W. -J. Park, B. C. Sung, and J. -W. Park, "The effect of SFCL on electric power grid with wind-turbine generation system," *IEEE Trans. Appl. Supercond.,* vol. 20, pp. 1177-1181, 2010.

[11] W. Paul, M. Chen, M. Lakner, J. Rhyner, D. Braun, W. Lanz, and, M. Kleimaier "Superconducting fault current limiter: applications, technical and economical benefits, simulations and test results," CIGRE, Paris, France, Tech. Rep. CIGRE SC 1, 2000.

[12] J. Pinto, J. Matthews, and G. Sarno, "Stealth technology for wind turbines," *IET radar, sonar & navigation,* vol. 4, pp. 126-133, 2010.

[13] W. -J Park, B. C. Sung, K. -B. Song, J. -W. Park, "Parameter optimization of SFCL with wind-turbine generation system based on its protective coordination," *IEEE Trans. Appl. Supercond.,* vol. 21, pp. 2153-2156, 2011.

[14] S.-M. Cho, H.-S. Shin, and J.-C. Kim, "Study on coordination of protective relays between primary feeder and interconnecting transformer grounded by SFCL of wind Farm," *IEEE Trans. Appl. Supercond.,* vol. 22, pp. 5500404-5500407, 2012.

[15] B. C. Sung, D. K. Park, J.-W. Park, and T. K. Ko, "Study on a series resistive SFCL to improve power system transient stability: modeling, simulation, and experimental verification," *IEEE Trans. Ind. Electron.,* vol. 56, pp. 2412-2419, 2009.

[16] B. C. Sung, D. K. Park, J.-W. Park, and T. K. Ko, " Study on optimal location of a resistive SFCL applied to an electric power grid," *IEEE Trans. Appl. Supercond.,* vol. 19, pp. 2048-2052, 2009.

[17] S. Alaraifi, M. E. Moursi, and H. Zeineldin, "Optimal allocation of HTS-FCL for power system security and stability enhancement," *IEEE Trans. Power Syst.,* vol. 28, pp. 4701-4711, 2013.

[18] X. Zhang, H. S. Ruiz, Z. Zhong, and T. A. Coombs, "Implementation of Resistive Type Superconducting Fault Current Limiters in Electrical Grids: Performance Analysis and Measuring of Optimal Locations," *Preprint available at* http://arxiv.org/abs/1508.01162.

[19] R. Wesche, "Temperature dependence of critical currents in superconducting Bi-2212/Ag wires," *Physica C,* vol. 246, pp. 186-194, 1995.

[20] E. J. Cukauskas and Laura H. Allen, "Critical current characteristics of composite thin films of Au and YBa2Cu3O7," *Physica C,* vol. 313, pp. 11-20, 1999.

[21] S. R. Currás, J. Viña, M. Ruibal, M. T. González, M. R. Osorio, J. Maza, J. A. Veira, and F. Vidal, "Normal-state resistivity versus critical current in YBa2Cu3O7-d thin films at high current densities," *Physica C,* vol. 372-376, pp. 1095-1098, 2002.

[22] C. Lacroix and F. Sirois, "Concept of a current flow diverter for accelerating the normal zone propagation velocity in 2G HTS coated conductors," *Supercond. Sci. Technol.,* vol. 27, p. 035003, 2014.

[23] M. F. Crommie and A. Zettl, "Thermal-conductivity anisotropy of single-crystal $Bi_2Sr_2CaCu_2O_8$," *Phys. Rev. B,* vol. 43, 408-412, 1991.

[24] J. Bock, F. Breuer, H. Walter, M. Noe, R. Kreutz, M. Kleimaier, K. H. Weck, and S. Elschener, "Development and successful testing of MCP BSCCO-2212 components for a 10 MVA resistive superconducting fault current limiter," *Supercond. Sci. Technol.,* vol. 17, p. S122, 2004.

[25] Z. Melhem, "High temperature superconductors (HTS) for energy applications," *Woodhead Publishing Ltd,* 2011.

[26] R. M. Strzelecki, "Power electronics in smart electrical energy networks," *Springer Science & Business Media,* 2008.

[27] C. Neumann and M. Kleimaier, “Benefits of SFCLs with regard to system layout,” *Contribution to Session Group 13, CIGRE,* 2000.